

A Self-Consistent Space-Domain Decomposition Method for QM/MM Computations of Protein Electrostatic Potentials

Jose A. Gascon,[†] Siegfried S. F. Leung,[†] Enrique R. Batista,[‡] and Victor S. Batista^{*,†}

*Department of Chemistry, Yale University, P.O. Box 208107,
New Haven, Connecticut 06520-8107, and Theoretical Division,
Los Alamos National Laboratory, Los Alamos, New Mexico 87545*

Received September 4, 2005

Abstract: This paper introduces a self-consistent computational protocol for modeling protein electrostatic potentials according to static point-charge model distributions. The protocol involves a simple space-domain decomposition scheme where individual molecular domains are modeled as Quantum-Mechanical (QM) layers embedded in the otherwise classical Molecular-Mechanics (MM) protein environment. ElectroStatic-Potential (ESP) atomic charges of the constituent molecular domains are computed, to account for mutual polarization effects, and iterated until obtaining a self-consistent point-charge model of the protein electrostatic potential. The novel protocol achieves quantitative agreement with full QM calculations in the description of electrostatic potentials of small polypeptides where polarization effects are significant, showing a remarkable improvement relative to the corresponding electrostatic potentials obtained with popular MM force fields. The capabilities of the method are demonstrated in several applications, including calculations of the electrostatic potential in the potassium channel protein and the description of protein–protein electrostatic interactions.

1. Introduction

The development of rigorous and practical methods for the accurate description of molecular electrostatic potentials is a subject of great interest,^{1–25} since the energetics of molecular processes is often dominated by electrostatic energy contributions.^{26–52} In particular, electrostatic interactions play a central role in a variety of molecular processes in biological molecules,^{26–29} including enzyme catalysis,^{30,31} electron transfer,^{32,33} proton transport,^{30,34–37} ion channels,^{38,39} docking and ligand binding,^{40–45} macromolecular assembly,^{46–50} and signal transduction.^{51,52} However, a rigorous and practical ab initio method to compute accurate electrostatic potentials of biological molecules has yet to be established.^{53–59} This paper introduces one such method, an approach to obtain static point-charge models of protein

electrostatic potentials by combining a novel iterative self-consistent space-domain decomposition scheme with conventional Quantum Mechanics/Molecular Mechanics (QM/MM) hybrid methods.

QM/MM hybrid methods partition the system into QM and MM layers,⁶⁰ offering an ideally suited approach for describing the polarization of a molecular domain due to the influence of the surrounding (protein) environment. Such a methodology models the electrostatic perturbation of the MM layer, on the QM domain, according to the static point-charge model distributions prescribed by MM force fields.^{61–66} However, it is widely recognized that standard MM force fields are not sufficiently accurate as to reproduce ab initio quality electrostatic potentials. Overcoming this problem requires extending MM force fields with an explicit description of polarization, an open problem that has been the subject of intense research over the past decade.^{1–25,67–70}

Significant effort has been focused on the development of both polarizable protein force fields^{6–15,67–70} and polariz-

* Corresponding author e-mail: victor.batista@yale.edu.

[†] Yale University.

[‡] Los Alamos National Laboratory.

able models for small molecules.^{15–25} While these methods are expected to become routine practice, no polarizable force field has so far been widely implemented for protein modeling. Parameters are still under development, and published applications are limited to those from the development groups. This is partly due to the inherent difficulty of the polarization problem and the fact that the behavior of polarizable force fields for flexible molecules (e.g., amino acids) has yet to be fully understood.²⁴ Also, the methods and software required to treat polarization are not as standardized as for the pairwise protein potentials. Finally, the increased complexity and expense of polarizable force fields make their applications to protein modeling justifiable only when introducing significant corrections.

Semiempirical QM approaches, based on linear-scaling methods, are nowadays capable of calculating molecular electrostatic potentials for systems as large as proteins.^{71–74} Comparisons to benchmark calculations, however, indicate that accurate calculations of electrostatic potentials would still require the development of more reliable semiempirical methods,^{75–77} a problem that remains a subject of much current research interest.^{78–81}

Considering the central role of electrostatic interactions in biological systems, it is therefore imperative to develop accurate, yet practical, approaches for describing molecular electrostatic potentials. To this end, the first objective is the development of a computational protocol capable of providing accurate electrostatic potentials for proteins in well-defined configurations. The protocol introduced in this paper addresses such a computational task by computing protein electrostatic potentials according to rigorous ab initio quantum chemistry methods. Under the new protocol, the protein is partitioned into molecular domains according to a simple space-domain decomposition scheme. ElectroStatic-Potential (ESP) atomic charges of the constituent domains are iteratively computed until reaching convergence in the description of the protein electrostatic potential. Such an iterative scheme scales linearly with the size the system, bypassing the enormous demands of memory and computational resources that would be required by a brute-force quantum chemistry calculation of the complete system. The accuracy and capabilities of the method are demonstrated in applications to benchmark calculations as well as in studies of the electrostatic potential in the potassium ion channel and electrostatic contributions to protein–protein interactions.

The paper is organized as follows. Section 2.1 describes the specific QM/MM methodology applied in this study. Section 2.2 describes the space-domain decomposition scheme for computations of electrostatic potentials. The computational details regarding the calculation of ESP charges are outlined in the Appendix. Results are presented in section 3, including applications to calculations of electrostatic potentials in the potassium channel protein and the description of protein–protein electrostatic interactions in the barnase–barstar complex, modeling solvation effects according to the Poisson–Boltzmann equation. Section 4 summarizes and concludes.

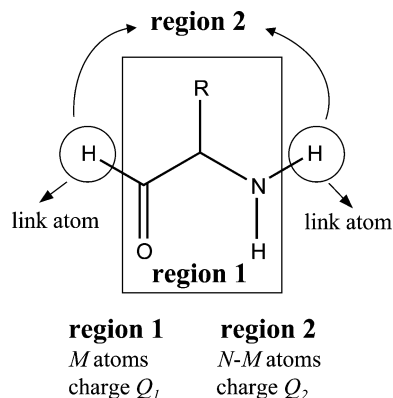


Figure 1. Representation of the regions used in the fitting procedure for each QM/MM calculation. Although a single residue is shown, region 1 may actually contain more than one residue.

2. Methods

2.1. QM/MM Methodology. The computational protocol, detailed in section 2.2, can be implemented in combination with any QM/MM hybrid method in which the polarization of the QM region due to the electrostatic influence of the surrounding molecular environment is explicitly considered. The particular QM/MM methodology applied in this study is the ONIOM-EE (HF/6-31G*:Amber) approach,^{82–88} as implemented in Gaussian03,⁸⁹ with QM and MM layers defined in Figure 1.⁹⁰

In the ONIOM-EE approach, the molecular domain of interest (herein called region *X*) is treated according to rigorous ab initio quantum chemistry methods, while the rest of the system (herein called region *Y*) is treated according to MM force fields. For systems where regions *X* and *Y* are covalently bonded, a QM/MM boundary is defined, and the covalency of frontier atoms is completed according to the standard link-hydrogen atom scheme.

The computation of a molecular property *A* (e.g., the energy, or the molecular electrostatic potential) involves the combination of three independent calculations:

$$A = A_{X+Y}(\text{MM}) + A_X(\text{QM}) - A_X(\text{MM}) \quad (1)$$

Here, $A_{X+Y}(\text{MM})$ is the property of interest, modeled at the MM level of theory for the complete system, while $A_X(\text{QM})$ and $A_X(\text{MM})$ are the same property of the reduced-system computed at the QM and MM levels of theory, respectively.

The effect of electrostatic interactions between the QM and MM layers is included in the calculation of both $A_X(\text{QM})$ and $A_X(\text{MM})$. In particular, $A_X(\text{QM})$ includes the effect of electrostatic interactions between the distribution of charges in the MM region and the electronic density of the QM layer obtained according to ab initio quantum chemistry methods. In addition, the contributions due to electrostatic interactions between regions *X* and *Y*, modeled at the MM level, are included in the calculation of both $A_X(\text{MM})$ and $A_{X+Y}(\text{MM})$ and therefore cancel out. The resulting evaluation of molecular properties thus includes a QM description of polarization of the reduced system, as influenced by the surrounding protein environment, while van der Waals interactions between *X* and *Y* are described at the MM level. For

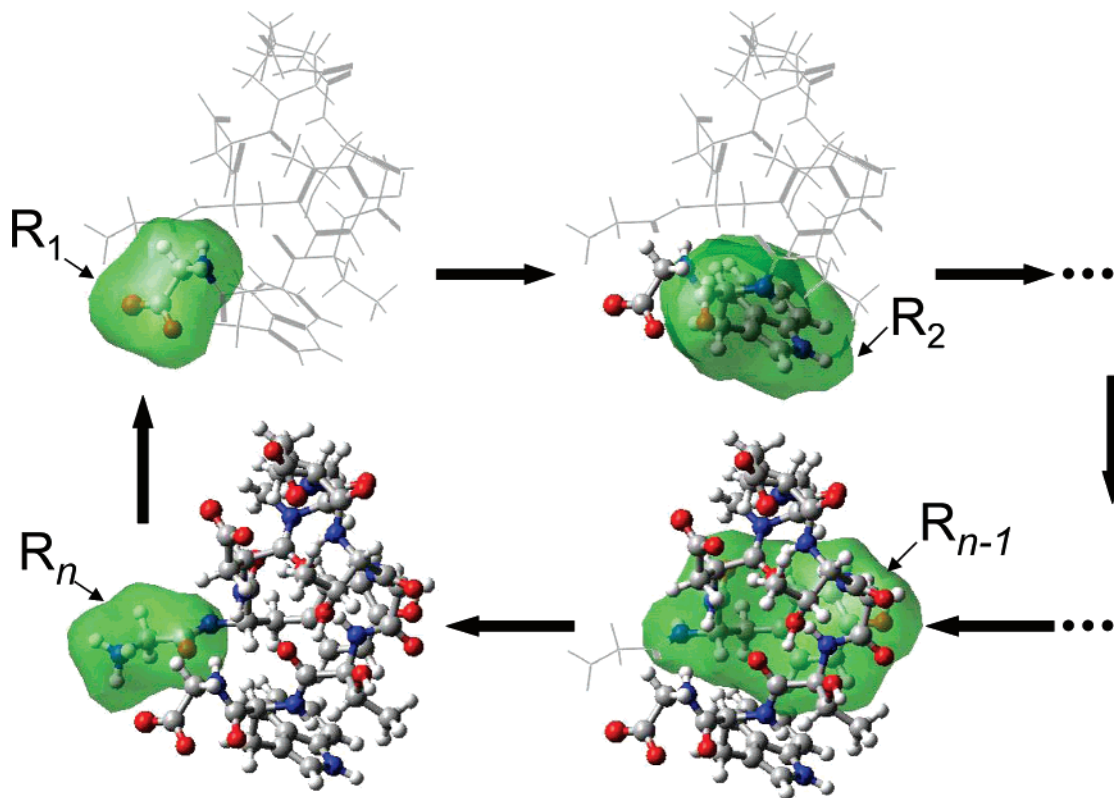


Figure 2. Representation of the MoD-QM/MM method. Green surfaces represent the QM region in QM/MM calculations. Colored balls and sticks represent regions with updated charges.

comparison, QM/MM calculations where the QM layer is *not* polarized by the surrounding environment are performed at the *ONIOM Molecular-Embedding* (ONIOM-ME) level of theory. In this QM/MM approach $A_X(\text{QM})$ and $A_X(\text{MM})$ do *not* include electrostatic interactions between regions X and Y .

Determination of ESP atomic charges is based on a least-squares minimization procedure where the electrostatic potential due to the ESP charges is fitted to the QM/MM electrostatic potential computed over a set of grid points around the QM layer. A detailed description of the calculation of ESP atomic charges, subject to the boundary conditions imposed by the link-hydrogen atom scheme, is presented in the Appendix.

2.2. Space-Domain Decomposition Scheme. Consider the task of modeling the molecular electrostatic potential of a polypeptide in a well-defined configuration (e.g., the X-ray structure). For a small polypeptide, such a calculation can be accomplished by first computing the molecular electronic density, according to rigorous *ab initio* quantum chemistry methods, and subsequently fitting the electrostatic potential on a set of grid points around the molecule to a standard multipole expansion.^{78,91–93}

The simplest model truncates the multipole expansion after the monopole term, thus requiring only the calculation of ESP atomic charges. While rigorous, such a calculation is computationally intractable for large systems (e.g., proteins) due to the overwhelming demands of memory and computational resources that would be required by ‘brute-force’ quantum chemistry calculations of the complete system. As a result, it is common practice to approximate protein

electrostatic potentials as a sum of the electrostatic potentials of the constituent molecular fragments (e.g., amino acid residues), neglecting the mutual polarization effects. Computations based on popular MM force fields^{61–66} as well as studies of protein docking^{42,48} or activity relationships^{94,95} are based on such an approximation, even though breakdown of this assumption is the rule rather than the exception whenever there are charged or polar fragments (e.g., amino acid residues) in the system. It would, therefore, prove a significant advance to extend such a methodology to compute distributions of ESP atomic charges where polarization effects are explicitly considered.

Motivated by the necessity to avoid a ‘brute-force’ quantum chemistry calculation of the complete system, an iterative space-domain decomposition scheme is introduced (see Figure 2): the system is partitioned into molecular domains (green regions in Figure 2) of suitable size for efficient quantum chemistry calculations. For simplicity, proteins are partitioned into n molecular domains containing amino acid residues R_1, R_2, \dots, R_n , although more general partitioning schemes could be considered analogously (e.g., partitions containing more than one residue, ions, and solvent molecules). The computation of the protein electrostatic potential can then be accomplished as follows. Starting with a QM layer containing amino acid residue R_1 (see top-left panel of Figure 2, green region), the ESP atomic charges of R_1 are computed according to the QM/MM hybrid methods that explicitly consider the electrostatic influence of the MM layer describing the surrounding protein environment. Next, the QM layer is redefined as a molecular domain containing amino acid residue R_2 (see top-right panel of Figure 2, green

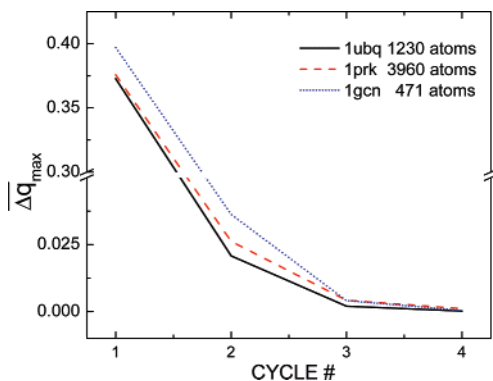


Figure 3. Maximum atomic charge difference (in atomic units) between successive iterations, averaged over all residues, as a function of the MoD-QM/MM iteration cycle. Three representative proteins are shown, including ubiquitin from *Human erythrocytes* (1ubq), proteinase K (2prk) from *Tritirachium album*, and glucagon (1gcn) from *Sus scrofa*.

region). The atomic charges of R_1 , now in the MM layer (balls and sticks, top-right panel of Figure 2), are updated according to the ESP charges obtained in the previous step. The ESP atomic charges of amino acid residue R_2 are computed analogously, and the procedure is subsequently applied to the remaining set of molecular domains containing amino acid residues $R_3 \dots R_n$. Note that each calculation of atomic charges considers the updated distribution of charges on all previously considered molecular domains. The entire computational cycle is subsequently iterated several times until reaching self-consistency.

The resulting methodology (called ‘Moving Domain-QM/MM’ (MoD-QM/MM) approach throughout this manuscript) converges within a few iteration cycles (i.e., usually 4 or 5 cycles), scaling linearly with the size of the system (i.e., the total computational time is $\tau = N_c \times \tau_0 \times n$, where $N_c \approx 4$ is the number of iteration cycles needed for convergence, τ_0 is the average computational time required for a single-point calculation of an individual molecular domain, typically a few minutes, and n is the number of molecular domains in the protein). The advantage of the resulting electrostatic potential, relative to other models based on static point-charge model distributions,^{61–66} is that the MoD-QM/MM approach explicitly considers mutual polarization effects between amino acid residues, providing ab initio quality electrostatic potentials (see section 3). The accuracy of the resulting molecular electrostatic potential, however, comes at the expense of *transferability* since the computed distribution of atomic charges is in principle *nontransferable* to other protein configurations. Therefore, while accurate, the computed electrostatic potential is useful only for applications where conformational changes are negligible.

Figure 3 illustrates typical convergence rates for the implementation of the MoD-QM/MM computational protocol, as applied to the calculation of the molecular electrostatic potentials of three representative protein structures downloaded from the Protein Data Bank, including Ubiquitin from *Human erythrocytes* (1ubq), solved at 1.8 Å resolution,⁹⁶ Proteinase K (2prk) from *Tritirachium album*, solved at 1.5 Å resolution,⁹⁷ and Glucagon (1gcn) from *Sus scrofa*, solved at 3.0 Å resolution.⁹⁸ Figure 3 shows a convergence measure

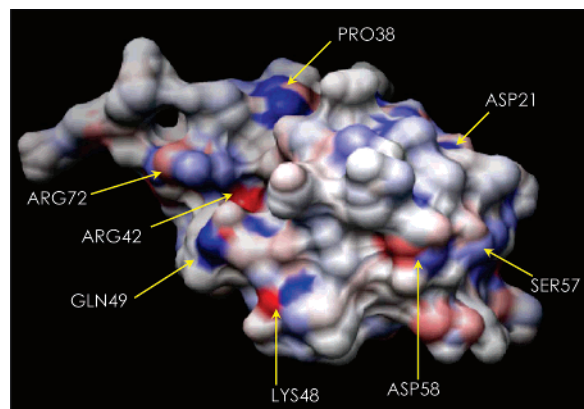


Figure 4. Surface of ubiquitin colored according to the differences in atomic charges obtained by considering, or neglecting, the mutual electrostatic influence between amino acid residues at the ONIOM-EE and ONIOM-ME levels of theory, respectively. Blue(red) color indicates an increase-(decrease) in electronic density due to polarization effects (maximum differences, indicated by bright coloring, correspond to changes of atomic charges of the order of $\pm 20\%$).

as a function of the iteration cycle, defined as the maximum change in atomic charges per residue averaged over all amino acid residues in the protein. It is shown that self-consistency is typically achieved within four iteration cycles, a convergence rate that is found to be independent of the system size. It is also found that the convergence rate is independent of the order chosen for treating individual molecular domains in each cycle.

To illustrate typical results of protein polarization, as modeled by the MoD-QM/MM protocol, Figure 4 shows a color map of the 1ubq surface displaying differences in atomic charges obtained by considering, or neglecting, the mutual electrostatic influence between amino acid residues at the ONIOM-EE and ONIOM-ME levels of theory, respectively. It is shown that typical corrections to atomic charges of specific amino acid residues can be as large as 20% due to polarization effects. These corrections are thus expected to be important in applications where there is collective electrostatic influence with contributions from several residues.

3. Results

Results are presented in three subsections. Section 3.1 demonstrates the capabilities of the MoD-QM/MM methodology for reproducing ab initio electrostatic potentials associated with the so-called ‘molecular bottleneck’ in the potassium channel protein from *streptomyces lividans*.⁹⁹ Section 3.2 implements the MoD-QM/MM method, in conjunction with the Poisson–Boltzmann equation, in applications to the description of protein–protein electrostatic interactions. Finally, section 3.3 analyzes the capabilities of the MoD-QM/MM method for generating a data bank of electrostatic potentials associated with several proteins in their X-ray structure configurations.

3.1. Potassium Ion Channel. This section illustrates the implementation of the MoD-QM/MM approach as applied to the description of the molecular electrostatic potential of

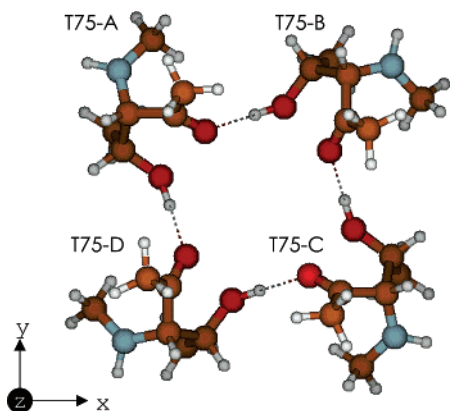


Figure 5. Structure of the complex formed by threonine residues (THR-75) of the four identical subunits forming the selectivity filter in the KcsA potassium channel.

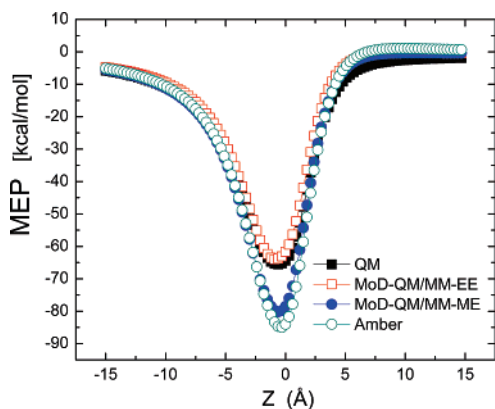


Figure 6. Molecular electrostatic potential (MEP) along the central axis of the tetramer of threonine residues (THR-75) in the KcsA potassium channel.⁹⁹ The MEP is calculated according to four different methods: full Quantum Mechanics at the HF/6-31G* level of theory (open square); atomic charges obtained with the MoD-QM/MM-EE approach (solid square); MoD-QM/MM at the ONIOM-ME (HF/6-31G*:Amber) level (i.e.: neglecting polarization) (solid circle); and Amber MM force field charges (open circle).

the potassium channel protein from *Streptomyces lividans* (KcsA K⁺ channel),^{39,99} with emphasis on benchmark calculations on truncated and QM/MM models of the so-called *selectivity filter*.

System (1) involves a truncated tetramer benchmark model amenable to rigorous ab initio quantum chemistry calculations (see Figure 5). The model involves 88 atoms and includes only the residues THR-75 belonging to the four identical peptide chains that constitute the ion channel. Such a tetramer provides the largest contribution to the molecular electrostatic potential at the selectivity filter. The structural model is built according to the configuration of the THR-75 tetramer in the X-ray crystal structure of the KcsA K⁺ channel (PDB access code 1bl8), adding hydrogen atoms and capping both ends of the THR residues with methyl groups. The MoD-QM/MM approach is implemented by partitioning the tetramer into four molecular domains defined by the individual THR-75 residues capped with methyl groups.

Figure 6 compares calculations of the electrostatic potential evaluated along the central axis of the ion channel (see Figure

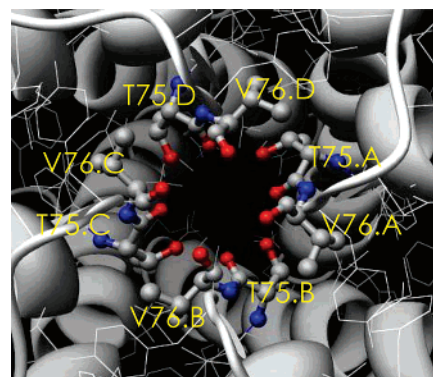


Figure 7. Structure of the complex formed by THR-75 and VAL-76 residues embedded in the KcsA potassium channel.

5, z-axis) according to four different methodologies, including the ab initio HF/6-31G* level, the MoD-QM/MM approach implemented at the ONIOM-EE (HF/6-31G*:Amber) level of theory (MoD-QM/MM-EE), and methods where polarization effects are neglected, including both the Amber MM force field and the MoD-QM/MM approach implemented at the ONIOM-ME (HF/6-31G*:Amber) level of theory (MoD-QM/MM-ME). The molecular electrostatic potential at position z is expressed in kcal/mol as the interaction energy felt by a unit of positive charge at position z . Figure 6 shows that the MoD-QM/MM-EE results are in excellent agreement with benchmark ab initio calculations. In contrast, calculations where polarization effects are neglected deviate strongly, overestimating the molecular electrostatic potential by more than 20 kcal/mol. In particular, the electrostatic potential obtained at the ONIOM-ME (HF/6-31G*:Amber) level of theory (i.e., neglecting mutual polarization effects between the four separate THR residues) is in very good agreement with the description provided by the Amber MM force field. These results indicate that deviations between ab initio and MM results are mainly due to the intrinsic approximation of MM force fields, based on transferable static point-charge model distributions that neglect polarization effects. Furthermore, the agreement between ab initio and MoD-QM/MM-EE calculations indicates that such polarization effects can be quantitatively addressed by the static point-charge model distributions generated according to the MoD-QM/MM-EE method, providing ab initio quality electrostatic potentials.

System (2) involves a QM/MM structural model of the complete KcsA K⁺ channel with an expanded QM layer of 128 atoms that includes both THR-75 and VAL-76 residues of the four identical polypeptide subunits forming the selectivity filter (see Figure 7). The rest of the protein is treated at the MM level. The model allows one to address the capabilities of the MoD-QM/MM computational protocol as applied to the description of polarization of an extended QM layer due to the influence of the surrounding protein environment.

The structural model of the entire protein is prepared according to the X-ray crystal configuration of the KcsA K⁺ channel (PDB access code 1bl8) adding hydrogens and partially relaxing the protein configuration, keeping α -carbons fixed at their crystallographic positions in order to

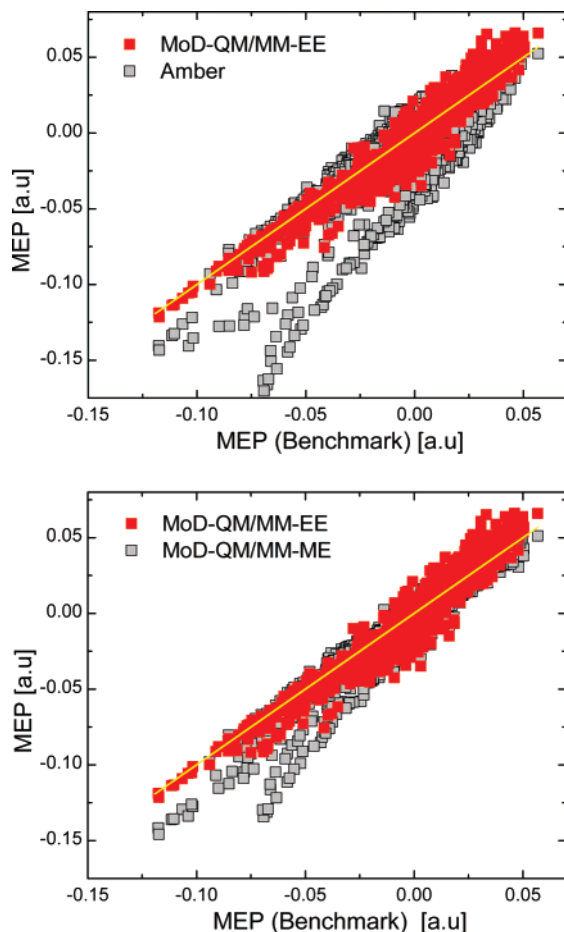


Figure 8. Correlation between the Molecular Electrostatic Potentials (MEP) (in atomic units) obtained according to the MoD-QM/MM-EE approach (red points) and benchmark QM/MM calculations for a distribution of grid of points around the tetramer of THR-75 and VAL-76 residues. The yellow line indicates complete correlation with benchmark calculations. The upper and lower panels compare the correlation of MEP obtained according to the MoD-QM/MM-EE approach (red points) with the corresponding results obtained by neglecting polarization effects according to the Amber MM force field (upper panel, gray points) and the MoD-QM/MM-ME method (lower panel, gray points).

preserve the natural shape of the protein. Benchmark calculations of the molecular electrostatic potential, computed at the ONIOM-EE (HF/6-31G*:Amber) level of theory, are compared to the corresponding results obtained according to the MoD-QM/MM-EE method, the Amber MM force field, and the MoD-QM/MM-ME approach. The MoD-QM/MM methodology is implemented by partitioning the system into four molecular domains. Each domain includes a THR-75/VAL-76 pair of residues with link hydrogen atoms placed at the amide bonds between THR-74 and THR-75 and between VAL-76 and GLY-77.

Figure 8 shows the correlation between MoD-QM/MM and benchmark QM/MM calculations of the electrostatic potential evaluated on a distribution of grid points away from the z axis of the potassium channel. The grid involves a lattice of 3000 points distributed in three layers at 2.5 grid points/Å around the extended tetramer of THR-75 and VAL-76 residues. For completeness, Figure 8 also includes the

analysis of correlations between benchmark ab initio calculations and the corresponding results obtained according to the Amber MM force field (upper panel, gray points) and the MoD-QM/MM-ME approach (see Figure 8, lower panel, gray points) where polarization effects are neglected.

Deviations relative to complete correlation are quantified over the set of N_g grid points in terms of the root-mean squared deviation

$$\xi = \left[\sum_{i=1}^{N_g} (u_i - U_i)^2 / N_g \right]^{1/2} \quad (2)$$

Here, U_i is the reference QM/MM electrostatic potential evaluated at grid point i and u_i is the electrostatic potential generated according to the static point-charge models generated by the MoD-QM/MM-EE, MoD-QM/MM-ME methods or the Amber MM force field. Root-mean-squared deviations $\xi = 4.9, 6.6,$ and 11.3 kcal/mol/C are obtained when using the MoD-QM/MM-EE, MoD-QM/MM-ME, and Amber MM force field methods, respectively. These results indicate that the MoD-QM/MM-EE approach correlates significantly better with benchmark calculations than methods where polarization effects are neglected.

3.2. Protein–Protein Interactions. The binding energy of protein–protein complexes often depends on a delicate balance of several factors, including hydrophobic and electrostatic energy contributions associated with protein–protein and solvent–protein interactions.¹⁰⁰ Computations based on continuum electrostatic methods¹⁰¹ suggest that even complementary Coulombic interactions that stabilize protein–protein complexes are usually not strong enough to compensate for unfavorable desolvation effects.^{102–107} Therefore, the driving force for complexation is generally expected to come mainly from nonpolar interactions.^{106,108} However, continuum electrostatic calculations are usually based on inaccurate molecular electrostatic potentials provided by nonpolarizable MM force fields. Therefore, it is natural to expect that calculations based on more accurate electrostatic potentials might provide further insight on the role played by electrostatic interactions in the process of protein–protein complexation.

This section applies the MoD-QM/MM approach in conjunction with the methods of continuum electrostatics in order to analyze the electrostatic contributions to the binding energy of the complex formed by the extracellular ribonuclease barnase and its intracellular inhibitor, the protein barstar. Such a complex system is ideally suited to investigate the capabilities of the MoD-QM/MM approach for explicitly modeling polarization effects because the complex has been extensively investigated both theoretically and experimentally.^{49,109–113}

The barnase–barstar complex involves complementary proteins that bind fast and with high affinity. The binding interface involves mainly polar and charged residues as well as several bound-water molecules stabilizing the complex through complementary electrostatic interactions. However, the desolvation energy of charged and polar residues destabilizes the complex. Previous theoretical studies, based on continuum solvent models,^{49,109–113} show contradictory

results regarding the analysis of stabilizing and destabilizing factors. Studies include reports of an unfavorable electrostatic binding energy of +14 kcal/mol,¹¹¹ a near zero electrostatic contribution to the binding energy (with desolvation and complexation terms almost canceling each other),⁴⁹ and finally, a favorable electrostatic contribution when considering a high protein dielectric constant.¹¹² The main objective of this section is to address this controversial aspect of the problem, recalculating the electrostatic contributions to the binding energy of the barnase–barstar complex according to the same methods of continuum electrostatics, using a distribution of atomic charges of the complex obtained according to the MoD-QM/MM-EE approach.

The structure of the barnase–barstar complex is prepared according to ref 49. The electrostatic contribution to the binding energy of complexation of barnase (A) and barstar (B) to form the barnase–barstar complex (AB) is defined as

$$\Delta\Delta G_{\text{elec}} = \Delta G_{\text{elec}}(AB) - \Delta G_{\text{elec}}(A) - \Delta G_{\text{elec}}(B) \quad (3)$$

where $\Delta G_{\text{elec}}(\xi)$ represents the electrostatic free-energy of the macromolecular system ξ

$$\Delta G_{\text{elec}}(\xi) = \frac{1}{2} \sum_i q_i \phi(\mathbf{r}_i) \quad (4)$$

where ξ is either A, B, or AB and the summation is carried out over all atomic charges q_i in ξ .

The electrostatic potential $\phi(\mathbf{r}_i)$, corresponding to charges q_i placed at \mathbf{r}_i , is obtained by solving the finite-difference Poisson–Boltzmann equation^{114,115} with Delphi.¹¹⁶ The interiors of the protein complex and aqueous solution are modeled as continuum media with dielectric constants $\epsilon_p = 2$ and $\epsilon_w = 80$, respectively. The choice of $\epsilon_p = 2$ for the dielectric constant of the protein interior is consistent with previous studies based on the assumption that complexation does not involve conformational changes but only electronic relaxation.⁴⁹ Boundary conditions are approximated by the Debye–Hückel potential of the charge distribution. The total energy calculations is converged within $10^{-4} k_B T$, where k_B is the Boltzmann constant and T is the absolute room-temperature. Atomic radii are defined according to the CHARMM MM force field.⁶⁶

The electrostatic contributions to the free-energy of complexation $\Delta\Delta G_{\text{elec}}$ is -12.6 kcal/mol, when using the distribution of atomic charges given by the MoD-QM/MM-EE protocol, with 0.1 M ionic strength of the aqueous solution and 1.4 \AA for the ionic exclusion radius, indicating significant electrostatic stabilization of the complex. In contrast, the electrostatic contributions computed by using the CHARMM distribution of atomic charges, where protein polarization effects are not explicitly considered, is $\Delta\Delta G_{\text{elec}} = 3.3$ kcal/mol, in agreement with previous calculations.⁴⁹ These results indicate that the overall electrostatic stabilization of the complex is mainly due to protein polarization over the extended protein–protein contact surface.

It has been recognized that the results of Poisson–Boltzmann calculations depend rather sensitively on the

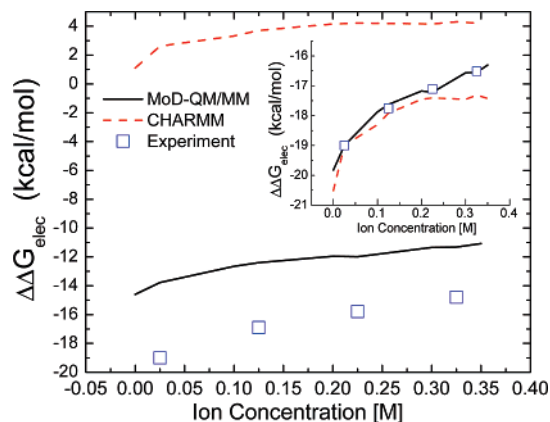


Figure 9. Calculated and experimental¹¹⁸ binding energies as a function of the ionic strength. The inset shows all curves artificially shifted to make them coincide at 25 mM, to facilitate the comparison of ionic strength dependency.

atomic radii. In fact, a set of atomic Born radii has been obtained by Roux and co-workers¹¹⁷ to reproduce quantitatively the electrostatic contributions to the solvation free energy of the 20 natural amino acids, computed by free energy perturbation techniques, performing Poisson–Boltzmann calculations with the CHARMM MM force field. Using such a set of atomic radii we obtain $\Delta\Delta G_{\text{elec}} = -3.3$ kcal/mol for 0.1 M ionic strength of the aqueous solution, when using the atomic charges prescribed by the CHARMM MM force field and $\Delta\Delta G_{\text{elec}} = -23.0$ kcal/mol when using the atomic charges obtained according to the MoD-QM/MM-EE protocol in close agreement with the experimental value $\Delta\Delta G_{\text{elec}} = -19.0$ kcal/mol.¹¹⁸

For completeness, Figure 9 compares experimental binding energies¹¹⁸ as a function of ionic strength and the corresponding electrostatic contributions to the binding energy computed by using the distribution of atomic charges provided by the MoD-QM/MM approach and the CHARMM MM force field. These results indicate that electrostatic interactions, as described by the MoD-QM/MM protocol, play a dominant role in the overall stabilization of protein complexes and reproduce the experimental dependence of the binding stability as a function of the solution ionic strength.

The observation that polarization effects play a dominant role in the overall stabilization of the complex barnase–barstar leads to the following questions: What residues are more significantly polarized? What are the specific interactions responsible for polarization of individual residues? To address these questions, a detailed analysis of electrostatic contributions is performed. The binding energy of the complex is recomputed, after substituting the polarized charges of individual residues obtained at the ONIOM-EE level by the unpolarized charges obtained at ONIOM-ME level of theory. The electrostatic contribution to the total binding energy of the complex, due to polarization of residue i , is then defined as the resulting change in binding energy $\Delta\Delta G_{\text{elec}}^i$.

The upper and lower panels of Figure 10 show the results of $\Delta\Delta G_{\text{elec}}^i$ for all residues in barnase and barstar, respectively. It is shown that the largest contribution to the binding

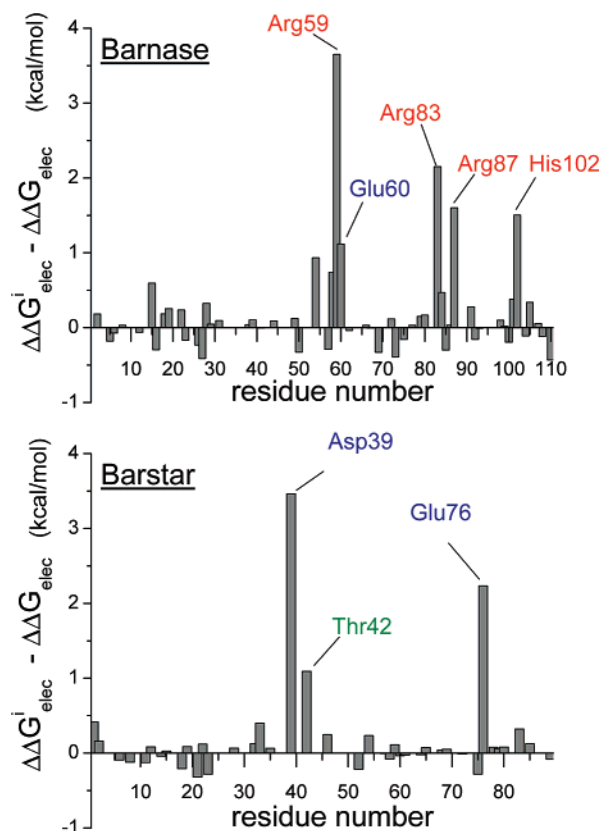


Figure 10. $\Delta\Delta G_{\text{elec}}^i$ in the upper and lower panels represents the binding energy of the complex after replacing the MoD-QM/MM-EE charges on residue i by MoD-QM/MM-ME charges. $\Delta\Delta G_{\text{elec}}$ is the binding energy as reported in the text (i.e. using MoD-QM/MM-EE charges for all residues).

energy due to polarization of individual residues in barnase results from the amino acid residues Arg-59, Arg-83, and Arg-87, while residues Asp-39 and Glu-76 provide the most important contributions in barstar. Not surprisingly, all of these residues are located at the complex interface and polarize each other through specific residue–residue interactions. In particular, Arg-83 and Arg-87 are polarized by Asp-39. Similarly Arg-59 forms a salt bridge with Glu-76. These results strongly suggest that the specific polarization of multiple pairs of amino acid residues at the barnase–barstar interface is largely responsible for the binding energy of the complex.

3.3. MM Force Fields. The calculations reported in previous sections illustrate the well-known fact that non-polarizable MM force fields (i.e., based on transferable static point-charge distributions) provide only approximate descriptions of molecular electrostatic potentials, commonly exhibiting significant deviations from benchmark *ab initio* calculations. In contrast, the static point-charge model distributions generated according to the MoD-QM/MM protocol are capable of providing more accurate electrostatic models, at least when the systems remain near the reference (e.g., X-ray structure) configurations. Considering that there is a wide range of applications where conformational changes can be neglected, it is important to consider whether the MoD-QM/MM protocol can be applied to generate a data bank of *ab initio* quality electrostatic potentials based on static point-

Table 1. Root Mean Square Deviation (RMSD) of Optimized Protein Structures Relative to the Crystal Structure^{a,b}

protein	Amber	MoD-QM/MM-EE	OPLS	PFF
1MAG	1.71	1.37		
1PI8	1.76	1.44		
1UBQ	1.97	1.85	2.08	1.97
2PRK	0.99	0.93	1.26	1.33
1PGX	2.32	1.97	4.1	4.02
1GCR	1.55	1.32	1.53	1.54
1GCN	5.08	2.12	4.14	3.77
1SSI	1.64	1.54	1.93	1.89
2RN2	2.11	1.79	1.92	1.54
1LTD	1.41	1.00		
average	2.06	1.53	2.43	2.29

^a Reference 119. ^b RMSD values are reported in Å for molecular structures obtained by using the Amber MM force field, the MoD-QM/MM-EE method, the Polarizable Force Field (PFF),¹¹⁹ and the OPLS MM force field.⁶⁵

charge model distributions, with emphasis on proteins at reference (e.g., X-ray structure) configurations. Furthermore, it is important to analyze whether such polarized static point-charge model distributions can be used to reparametrize standard MM force fields in an effort to improve their description of electrostatic potentials of specific proteins near their corresponding reference configurations.

Reparametrization of the Amber MM force field according to the distribution of atomic charges generated by the MoD-QM/MM protocol would, in principle, require a subsequent readjustment of the torsional coefficients.⁶⁴ In practice, however, torsional parameters are expected to remain almost unchanged so long as the minimum energy configuration is sufficiently similar to the reference (e.g., X-ray) structure. It is, therefore, expected that an approximate MM force field constructed by substituting the Amber charges by the atomic charges generated according to the MoD-QM/MM protocol could be sufficiently accurate as to provide a reliable description of both electrostatic and steric interactions whenever the system remains near the reference configuration.

To investigate the effect of charge reparametrization as applied to the Amber MM force field, 10 realistic protein structures from the Protein Data Bank (listed in Table 1) were used as initial geometries for gas-phase energy minimization after substituting the original RESP charges by ESP atomic charges generated according to the MoD-QM/MM protocol.

Table 1 shows the root-mean-square deviations (RMSD) relative to reference X-ray structures. For comparison, results obtained with four different approaches are shown, including the Amber MM force field, as parametrized with RESP charges; the Amber MM force field with atomic charges computed according to the MoD-QM/MM-EE protocol; the OPLS-AA MM force field;⁶⁵ and finally, results obtained with a Polarizable Force field (PFF).¹¹⁹ In all cases, geometry minimization procedures were performed using a convergence criterion of 0.05 kcal/mol/Å for the root-mean-square gradient. Since these proteins were resolved at a high resolution, it is reasonable to expect a low RMSD to be an

indication of how well the resulting force field describes the corresponding reference configurations. Table 1 shows that the RMSD obtained by using the Amber MM force field with MoD-QM/MM-EE atomic charges favorably compares to other alternative approaches. While still approximate, the resulting modified force field is thus expected to provide not only better quality electrostatic potentials than those provided by the original MM force field but also minimum energy configurations more similar to the reference X-ray crystal structures.

4. Conclusions

We have introduced the MoD-QM/MM computational protocol to account for protein polarization effects when computing molecular electrostatic potentials according to static point-charge model distributions. The method implements an iterative space-domain decomposition scheme, partitioning the protein into molecular domains of suitable size for efficient quantum chemistry calculations. ESP atomic charges are then computed, in a self-consistent manner, according to QM/MM hybrid methods that explicitly include polarization effects due to the electrostatic influence of the surrounding protein environment. The resulting methodology usually converges within a few iteration cycles, regardless of the protein size. Therefore, the overall computational cost scales *linearly* with the size of the system, bypassing the enormous demands of computational resources that would be required by brute-force quantum chemistry calculations of the complete protein.

We have shown that quantitative agreement with *ab initio* calculations is verified in the description of electrostatic potentials of small polypeptides benchmark systems where polarization effects are significant, showing a remarkable improvement relative to the corresponding electrostatic potentials obtained with popular MM force fields. Furthermore, the application of the MoD-QM/MM method to the QM/MM description of the potassium channel of *streptomyces lividans* demonstrates the capabilities of the protocol for modeling polarization effects induced by the surrounding protein environment on the selectivity filter.

We showed that the MoD-QM/MM protocol, implemented in conjunction with methods of continuum electrostatics, offers a particularly promising methodology for studies of protein–protein interactions where protein polarization effects are explicitly considered. The application of such a combined methodology to calculations of electrostatic contributions to the binding energy of the barnase–barstar complex indicates that polarization of the protein–protein interface can lead to significant electrostatic stabilization of the complex. Furthermore, we have shown that such an electrostatic contribution is most responsible for the overall dependency of the total binding free-energy with ionic strength.

We have demonstrated the feasibility of constructing a data bank of electrostatic potentials based on static point-charge model distributions corresponding to protein structures from the Protein Data Bank. Finally, we have implemented the generated electrostatic potentials in conjunction with the Amber MM force field in an effort to improve the description

of electrostatic potentials provided by MM force fields and generate relaxed minimum energy configurations more similar to reference high-resolution X-ray crystal structures.

Acknowledgment. V.S.B. acknowledges a generous allocation of supercomputer time from the National Energy Research Scientific Computing (NERSC) center and financial support from Research Corporation, Research Innovation Award # RI0702, a Petroleum Research Fund Award from the American Chemical Society PRF # 37789- G6, a junior faculty award from the F. Warren Hellman Family, the National Science Foundation (NSF) Career Program Award CHE # 0345984, the NSF Nanoscale Exploratory Research (NER) Award ECS # 0404191, the Alfred P. Sloan Fellowship (2005–2006), a Camille Dreyfus Teacher-Scholar Award for 2005, and a Yale Junior Faculty Fellowship in the Natural Sciences (2005–2006). S.S.F.L. acknowledges a summer research fellowship and hospitality at LANL and support from the NIH predoctoral training grant T32 GM008283. S.S.F.L. and E.R.B. acknowledge funding from the LDRD program at LANL and the Heavy element chemistry BES-DOE program. The authors are grateful to Mr. Sabas Abuabara for proofreading the manuscript.

Appendix: QM/MM Computation of ESP Atomic Charges

This section describes the implementation of boundary conditions imposed by the link-hydrogen atom scheme for computations of ESP atomic charges of an individual amino acid residue, as polarized by the surrounding protein environment.

For a given QM/MM calculation, N is the total number of atoms in the QM layer, including M atoms within the residue and $N - M$ link atoms (see Figure 1). The total charge of the QM layer is

$$Q = Q_1 + Q_2 \quad (\text{A-1})$$

where

$$Q_1 = \sum_{i=1}^{M-1} q_i + q_M, \quad Q_2 = \sum_{i=M+1}^{N-1} q_i + q_N \quad (\text{A-2})$$

where Q_1 is the net charge of the residue and Q_2 is set equal to zero in order to ensure consistency with standard MM force fields.

The electrostatic potential at position \mathbf{r}_j due to all point charges in the QM region is written as

$$u_j = \sum_{i=1}^N \frac{q_i}{r_{ji}} \quad (\text{A-3})$$

where $r_{ji} \equiv |\mathbf{r}_j - \mathbf{r}_i|$. Since we impose conditions (A-2) for the charge in regions 1 and 2, eq A-3 can be written as follows:

$$u_j = \sum_{i=1}^{M-1} \left[\frac{q_i}{r_{ji}} - \frac{q_i}{r_{jM}} \right] + \frac{Q_1}{r_{jM}} + \sum_{i=M+1}^{N-1} \left[\frac{q_i}{r_{ji}} - \frac{q_i}{r_{jN}} \right] + \frac{Q_2}{r_{jN}} \quad (\text{A-4})$$

Making the substitutions, $F_{jik} \equiv (1/r_{ji} - 1/r_{jk})$ and $K_{jk} \equiv 1/r_{jk}$, eq A-4 can be rewritten as follows:

$$u_j = \sum_{i=1}^{M-1} q_i F_{jiM} + \sum_{i=M+1}^{N-1} q_i F_{jiN} + Q_1 K_{jM} + Q_2 K_{jN} \quad (\text{A-5})$$

The actual computation of ESP atomic charges q_i requires a least-squares minimization of the χ^2 error function

$$\chi^2 = \sum_j^{N_g} (u_j - U_j)^2 \quad (\text{A-6})$$

where U_j is the QM/MM electrostatic potential at grid point j and u_j is the corresponding electrostatic potential defined by the distribution of point charges. The summation, introduced by eq A-6, is carried over a set of N_g grid points, associated with four layers of grid points at 1.4, 1.6, 1.8, and 2.0 times the van der Waals radii around the QM region, each of them with a density of 1 grid point \AA^{-2} .

From eq A-6, the minimum of χ^2 can be obtained by imposing the condition

$$\frac{\partial \chi^2}{\partial q_k} = - \sum_{j=1}^{N_g} 2(u_j - U_j) \frac{\partial u_j}{\partial q_k} = 0 \quad (\text{A-7})$$

for all q_k in the set $(q_1, \dots, q_{M-1}, q_{M+1}, \dots, q_{N-1})$. Further, eq A-5 indicates that $\partial u_j / \partial q_k = F_{jks}$, where s corresponds to M or N , depending on whether $k < M$ or $M < k < N$, respectively. Thus, eq A-7 can be rewritten as follows:

$$\sum_{j=1}^{N_g} [U_j - (Q_1 K_{jM} + Q_2 K_{jN})] F_{jks} = \sum_{i=1}^{M-1} q_i \sum_{j=1}^{N_g} F_{jiM} F_{jks} - \sum_{i=M+1}^{N-1} q_i \sum_{j=1}^{N_g} F_{jiN} F_{jks} \quad (\text{A-8})$$

Considering all possible q_k , eq A-8 is better represented in matrix notation as

$$\mathbf{c} = \mathbf{a} \begin{bmatrix} \mathbf{B}_1 & 0 \\ 0 & \mathbf{B}_2 \end{bmatrix} \quad (\text{A-9})$$

where, $c^k = \sum_{j=1}^{N_g} [U_j - (Q_1 K_{jM} + Q_2 K_{jN}) F_{jks}]$, $\mathbf{a} = (q_1, \dots, q_{M-1}, q_{M+1}, \dots, q_{N-1})$, $\mathbf{B}_1^{ik} = \sum_{j=1}^{N_g} F_{jiM} F_{jks}$, and $\mathbf{B}_2^{ik} = \sum_{j=1}^{N_g} F_{jiN} F_{jks}$. Note that vector \mathbf{c} and matrix \mathbf{B} are only functions of the electrostatic potential U_j evaluated at the grid points ($j = 1 \dots N_g$), the distances between atomic positions the grid points, r_{jk} and the partial charges Q_1 and Q_2 . Therefore, the atomic charges (\mathbf{a}) can be obtained by inversion of eqs A-9 and A-2.

Note Added after ASAP Publication. This article was inadvertently released ASAP on November 18, 2005 before several text corrections were made. The correct version was posted on December 5, 2005.

References

(1) van-der Vaart, A.; Bursulaya, B.; Brooks, C.; Merz, K. *J. Phys. Chem. B* **2000**, *104*, 9554–9563.

(2) Halgren, T.; Damm, W. *Curr. Opin. Struct. Biol.* **2001**, *11*, 236–242.

(3) Roux, B.; Berneche, S. *Biophys. J.* **2002**, *82*, 1681–1684.

(4) Rick, S. W.; Stuart, S. J. *Rev. Comput. Chem.* **2002**, *18*, 89–146.

(5) Ponder, J.; Case, D. A. *Adv. Prot. Chem.* **2003**, *66*, 27–47.

(6) Cieplak, P.; Caldwell, J.; Kollman, P. *J. Comput. Chem.* **2001**, *22*, 1048–1057.

(7) Banks, J. L.; Kaminski, G. A.; Zhou, R.; Mainz, D. T.; Berne, B. J.; Friesner, R. A. *J. Chem. Phys.* **1999**, *110*, 741–754.

(8) Stern, H. A.; Kaminski, G. A.; Banks, J.; Zhou, R.; Berne, B. J.; Friesner, R. A. *J. Phys. Chem. B* **1999**, *103*, 4730–4737.

(9) Gresh, N. *J. Phys. Chem. A* **1997**, *101*, 8680–8694.

(10) Masella, M.; Gresh, N.; Flament, J. P. *J. Chem. Soc., Faraday Trans.* **1998**, *94*, 2745–2753.

(11) Gresh, N.; Tiraboschi, G.; Salahub, D. R. *Biopolymers* **1998**, *45*, 405–425.

(12) Hermida-Ramon, J. M.; Brdarski, S.; Karlstrom, G.; Berg, U. *J. Comput. Chem.* **2003**, *24*, 161–176.

(13) Palmo, K.; Mannfors, B.; Mirkin, N. G.; Krimm, S. *Biopolymers* **2003**, *68*, 383–394.

(14) Palmo, K.; Krimm, S. *J. Comput. Chem.* **1998**, *19*, 754–768.

(15) Mannfors, B. E.; Mirkin, N. G.; Palmo, K.; Krimm, S. *J. Phys. Chem. A* **2003**, *107*, 1825–1832.

(16) Barnes, P.; Finney, J. L.; Nicholas, J. D.; Quinn, J. E. *Nature* **1979**, *282*, 459–464.

(17) Stillinger, F. H.; David, C. W. *J. Chem. Phys.* **1978**, *69*, 1473–1484.

(18) Corongiu, G. *Int. J. Quantum Chem.* **1992**, *42*, 1209–1235.

(19) Sprik, M.; Klein, M. L. *J. Chem. Phys.* **1988**, *89*, 7556–7560.

(20) Bernardo, D. N.; Ding, Y.; Krogh-Jespersen, K.; Levy, R. M. *J. Phys. Chem.* **1994**, *98*, 4180–4187.

(21) Yu, H.; Hansson, T.; van Gunsteren, W. F. *J. Chem. Phys.* **2003**, *118*, 221–234.

(22) Saint-Martin, H.; Hernandez-Cobos, J.; Bernal-Uruchurtu, M. I.; Ortega-Blake, I.; Berendsen, H. J. C. *J. Chem. Phys.* **2000**, *113*, 10899–10912.

(23) Stern, H. A.; Rittner, F.; Berne, B. J.; Friesner, R. A. *J. Chem. Phys.* **2001**, *115*, 2237–2251.

(24) Ren, P.; Ponder, J. W. *J. Phys. Chem. B* **2003**, *107*, 5933–5947.

(25) Burnham, C. J.; Xantheas, S. S. *J. Chem. Phys.* **2002**, *116*, 1479–1492.

(26) Perutz, M. *Science* **1978**, *201*, 1187–1191.

(27) Warshel, A. *Acc. Chem. Res.* **1981**, *14*, 284–290.

(28) Sharp, K.; Honig, B. *Annu. Rev. Biophys. Biophys. Chem.* **1990**, *19*, 301–332.

(29) Nakamura, H. *Q. Rev. Biophys.* **1996**, *29*, 1–90.

(30) Warshel, A. In *Computer modeling of chemical reactions in enzymes and solutions*; John Wiley & Sons: New York, 1991; pp 209–211, 225–228.

(31) Gascon, J.; Batista, V. *Biophys. J.* **2004**, *87*, 2931–2941.

- (32) Gunner, M.; Nichols, A.; Honig, B. *J. Chem. Phys.* **1996**, *100*, 4277–4291.
- (33) Parson, W. *Photosynth. Res.* **2003**, *76*, 81–92.
- (34) Sham, Y.; Muegge, I.; Warshel, A. *Proteins* **1999**, *36*, 484–500.
- (35) Okamura, M.; Feher, G. *Annu. Rev. Biochem.* **1992**, *61*, 861–896.
- (36) Popovic, D.; Stuchebrukhov, A. *J. Am. Chem. Soc.* **2004**, *126*, 1858–1871.
- (37) Burykin, A.; Warshel, A. *FEBS Lett.* **2004**, *570*, 41–46.
- (38) Aqvist, J.; Luzhkov, V. *Nature* **2000**, *404*, 881–884.
- (39) Bliznyuk, A.; Rendell, A.; Allen, T.; Chung, S. *J. Phys. Chem. B* **2001**, *105*, 12674–12679.
- (40) Simonson, T.; Archontis, G.; Karplus, M. *J. Phys. Chem. B* **1997**, *101*, 8349–8362.
- (41) Simonson, T.; Archontis, G.; Karplus, M. *J. Phys. Chem. B* **1999**, *103*, 6142–6156.
- (42) Muegge, I.; Rarey, M. Small molecule docking and scoring. In *Reviews in Computational Chemistry*; Lipkowitz, K., Boyd, D., Eds.; Wiley-VCH: New York, 2001; pp 1–60.
- (43) Vasilyev, V.; Bliznyuk, A. *Theor. Chem. Acc.* **2004**, *112*, 313–317.
- (44) Grater, F.; Schwarzl, S.; Dejaegere, A.; Fischer, S.; Smith, J. *J. Phys. Chem. B* **2005**, *109*, 10474–10483.
- (45) Cho, A.; Guallar, V.; Berne, B.; Friesner, R. *J. Comput. Chem.* **2005**, *26*, 915–931.
- (46) Andre, I.; Kesvatera, T.; Jonsson, B.; Akerfeldt, K.; Linse, S. *Biophys. J.* **2004**, *87*, 1929–1938.
- (47) Sheinerman, F. B.; Norel, R.; Honig, B. *Curr. Opin. Struct. Biol.* **2000**, *10*, 153–159.
- (48) Ehrlich, L. Protein–Protein Docking. In *Reviews in Computational Chemistry*; Lipkowitz, K., Boyd, D., Eds.; Wiley-VCH: New York, 2001; pp 61–97.
- (49) Sheinerman, F. B.; Honig, B. *J. Mol. Biol.* **2002**, *318*, 161–177.
- (50) Veselovsky, A.; Ivanov, Y.; Ivanov, A.; Archakov, A.; Lewi, P.; Janssen, P. *J. Mol. Recognit.* **2002**, *15*, 405–422.
- (51) Klahn, M.; Schlitter, J.; Gerwert, K. *Biophys. J.* **2005**, *88*, 3829–3844.
- (52) Warshel, M. S. A. S. A. *Proc. Natl. Acad. Sci.* **2003**, *100*, 14834–14839.
- (53) Nakano, T.; Kaminuma, T.; Sato, T.; Akiyama, Y.; Uebayasi, M.; Kitaura, K. *Chem. Phys. Lett.* **2000**, *318*, 614–618.
- (54) Nakano, T.; Kaminuma, T.; Sato, T.; Fukuzawa, K.; Akiyama, Y.; Uebayasi, M.; Kitaura, K. *Chem. Phys. Lett.* **2002**, *351*, 475–480.
- (55) Exner, T.; Mezey, P. *J. Phys. Chem. A* **2002**, *106*, 11891–11800.
- (56) Gao, A.; Zhang, D.; Zhang, J.; Zhang, Y. *Chem. Phys. Lett.* **2004**, *394*, 293–297.
- (57) Exner, T.; Mezey, P. *J. Phys. Chem. A* **2004**, *108*, 4301–4309.
- (58) Mei, Y.; Zhang, D.; Zhang, J. *J. Phys. Chem. A* **2005**, *109*, 2–5.
- (59) Li, S.; Fang, T. *J. Am. Chem. Soc.* **2005**, *127*, 7215–7226.
- (60) Warshel, A.; Levitt, M. *J. Mol. Biol.* **1976**, *103*, 227–249.
- (61) Halgren, T.; Damm, W. *Curr. Opin. Struct. Biol.* **2001**, *11*, 236–242.
- (62) Dykstra, C. *Chem. Rev.* **1993**, *93*, 2339–2353.
- (63) Wang, W.; Donini, O.; Reges, C.; Kollman, P. *Annu. Rev. Biophys. Biomol. Struct.* **2001**, *30*, 211–243.
- (64) Cornell, W. D.; Cieplak, P.; Bayly, C. I.; Gould, I. R.; Merz, K. M.; Ferguson, D. M.; Spellmeyer, D. C.; Fox, T.; Caldwell, J. W.; Kollman, P. A. *J. Am. Chem. Soc.* **1995**, *117*, 5179–5197.
- (65) Jorgensen, W.; Tirado-Rives, J. *J. Am. Chem. Soc.* **1988**, *110*, 1657–1666.
- (66) Brooks, B. R.; Brucoleri, R. E.; Olafson, B. D.; States, D. J.; Swaminathan, S.; Karplus, M. *J. Comput. Chem.* **1983**, *4*, 187–217.
- (67) Field, M. *Mol. Phys.* **1997**, *91*, 835–846.
- (68) Piquemal, J.; Williams-Hubbard, B.; Fey, N.; Deeth, R.; Gresh, N.; Giessner-Prettre, C. *J. Comput. Chem.* **2003**, *24*, 1963–1970.
- (69) Piquemal, J.; Gresh, N.; Giessner-Prettre, C. *J. Phys. Chem. A* **2003**, *107*, 10353–10359.
- (70) Maple, J.; Cao, Y.; Damm, W.; Halgren, T.; Kaminski, G.; Zhang, L.; Friesner, R. *J. Chem. Theory Comput.* **2005**, *1*, 694–715.
- (71) York, D.; Lee, T.; Yang, W. *J. Am. Chem. Soc.* **2005**, *127*, 7215–7226.
- (72) Stewart, J. *Int. J. Quantum Chem.* **1996**, *58*, 133–146.
- (73) Stewart, J. Mopac2000; Fujitsu Ltd.: Tokyo, 1999.
- (74) Cummins, P.; Gready, J. In *Hybrid Quantum Mechanical and Molecular Mechanical Methods*; Gao, J., Thompson, M., Eds.; American Chemical Society: Washington, DC, 1998; pp 250–263.
- (75) Zuegg, J.; Bliznyuk, A.; Gready, J. *Mol. Phys.* **2003**, *101*, 2437–2450.
- (76) Titmuss, S.; Cummins, P.; Rendell, A.; Bliznyuk, A.; Gready, J. *J. Comput. Chem.* **2002**, *23*, 1314–1322.
- (77) Titmuss, S.; Cummins, P.; Bliznyuk, A.; Rendell, A.; Gready, J. *Chem. Phys. Lett.* **2000**, *320*, 169–176.
- (78) Williams, D. Net atomic charge and multipole models for ab initio molecular electric potential. In *Reviews in Computational Chemistry*; Lipkowitz, K., Boyd, D., Eds.; Wiley-VCH: New York, 1991; pp 219–271.
- (79) Stewart, J. Semiempirical molecular orbital methods. In *Reviews in Computational Chemistry*; Lipkowitz, K., Boyd, D., Eds.; Wiley-VCH: New York, 1990; pp 45–81.
- (80) Zerner, M. Semiempirical molecular orbital methods. In *Reviews in Computational Chemistry*; Lipkowitz, K., Boyd, D., Eds.; Wiley-VCH: New York, 1991; pp 313–365.
- (81) Repasky, M.; Chandrasekar, J.; Jorgensen, W. *J. Comput. Chem.* **2002**, *23*, 1601–1622.
- (82) Maseras, M.; Morokuma, K. *J. Comput. Chem.* **1995**, *16*, 1170–1179.
- (83) Svensson, M.; Humbel, S.; Froese, R. D. J.; Matsubara, T.; Sieber, S.; Morokuma, K. *J. Phys. Chem.* **1996**, *100*, 19357–19363.
- (84) Humbel, S.; Sieber, S.; Morokuma, K. *J. Chem. Phys.* **1996**, *104*, 1959–1967.

- (85) Dapprich, S.; Komaromi, K.; Byun, K.; Morokuma, K.; Frisch, M. *J. Mol. Struct. (Theochem)* **1999**, *461*, 1–21.
- (86) Vreven, T.; Morokuma, K. *J. Comput. Chem.* **2000**, *21*, 1419–1432.
- (87) Vreven, T.; Mennucci, B.; daSilva, C. O.; Morokuma, K.; Tomasi, J. *J. Chem. Phys.* **2001**, *115*, 62–72.
- (88) Vreven, T.; Morokuma, K. *Theor. Chem. Acc.* **2003**, *109*, 125–132.
- (89) Frisch, M. J.; Trucks, G. W.; Schlegel, H. B.; Scuseria, G. E.; Robb, M. A.; Cheeseman, J. R.; Montgomery, J. A., Jr.; Vreven, T.; Kudin, K. N.; Burant, J. C.; Millam, J. M.; Iyengar, S. S.; Tomasi, J.; Barone, V.; Mennucci, B.; Cossi, M.; Scalmani, G.; Rega, N.; Petersson, G. A.; Nakatsuji, H.; Hada, M.; Ehara, M.; Toyota, K.; Fukuda, R.; Hasegawa, J.; Ishida, M.; Nakajima, T.; Honda, Y.; Kitao, O.; Nakai, H.; Klene, M.; Li, X.; Knox, J. E.; Hratchian, H. P.; Cross, J. B.; Adamo, C.; Jaramillo, J.; Gomperts, R.; Stratmann, R. E.; Yazyev, O.; Austin, A. J.; Cammi, R.; Pomelli, C.; Ochterski, J. W.; Ayala, P. Y.; Morokuma, K.; Voth, G. A.; Salvador, P.; Dannenberg, J. J.; Zakrzewski, V. G.; Dapprich, S.; Daniels, A. D.; Strain, M. C.; Farkas, O.; Malick, D. K.; Rabuck, A. D.; Raghavachari, K.; Foresman, J. B.; Ortiz, J. V.; Cui, Q.; Baboul, A. G.; Clifford, S.; Cioslowski, J.; Stefanov, B. B.; Liu, G.; Liashenko, A.; Piskorz, P.; Komaromi, I.; Martin, R. L.; Fox, D. J.; Keith, T.; Al-Laham, M. A.; Peng, C. Y.; Nanayakkara, A.; Challacombe, M.; Gill, P. M. W.; Johnson, B.; Chen, W.; Wong, M. W.; Gonzalez, C.; Pople, J. A. *Gaussian 03, Revision A.1*; 2003.
- (90) The choice of basis set and level of theory aims to make contact with earlier work, where the HF/6-31G* level of theory has been the standard for calculations of ESP atomic charges. For example, Peter Kollman and co-workers obtained ESP and RESP charges in the early parametrization of Amber (Cornell et al. *J. Am. Chem. Soc.* **1993**, *115*, 9620; *J. Am. Chem. Soc.* **1995**, *117*, 5179), and they showed that the HF/6-31G* level was able to reproduce experimental free energies of solvation. In the particular case of ion channels we used this level of theory to present a consistent comparison to the electrostatic potential provided by Amber. However, it is important to note that the proposed methodology is not limited to any particular basis set or level of quantum chemistry.
- (91) Politzer, P.; Murray, J. *Molecular Electrostatic Potentials and Chemical Reactivity*. In *Reviews in Computational Chemistry*; Lipkowitz, K., Boyd, D., Eds.; Wiley-VCH: New York, 1991; pp 273–312.
- (92) Murray, J.; Politzer, P. *Electrostatic Potentials: Chemical Applications*. In *The Encyclopedia of Computational Chemistry*; Schleyer, P., Allinger, N., Clark, T., Gasteiger, J., Kollman, P., Schaefer, H., Schreiner, P., Eds.; Wiley & Sons: Chichester, U.K., 1998; pp 912–920.
- (93) Murray, J.; Politzer, P. *The Molecular Electrostatic Potential: A Tool for Understanding and Predicting Molecular Interactions*. In *Molecular Orbital Calculations for Biological Systems*; Sapse, A.-M., Ed.; Oxford University Press: New York, 1998; pp 49–84.
- (94) Oprea, T.; Waller, C. *Theoretical and Practical Aspects of Three-Dimensional Quantitative Structure-Activity Relationships*. In *Reviews in Computational Chemistry*; Lipkowitz, K., Boyd, D., Eds.; Wiley-VCH: New York, 1997; pp 127–182.
- (95) Greco, G.; Novellino, E.; Martin, Y. *Approaches to Three-Dimensional Quantitative Structure-Activity Relationships*. In *Reviews in Computational Chemistry*; Lipkowitz, K., Boyd, D., Eds.; Wiley-VCH: New York, 1997; pp 183–240.
- (96) Vdaykumar, S.; Bugg, C.; Cook, W. *J. Mol. Biol.* **1987**, *194*, 531–544.
- (97) Betzel, C.; Pal, G.; Saenger, W. *Acta Crystallogr. B* **1988**, *44*, 163–172.
- (98) Sasaki, K.; Dockerill, S.; Adamiak, D.; Tickle, I.; Blundell, T. *Nature* **1975**, *257*, 751–757.
- (99) Doyle, D. A.; Cabral, J. M.; Pfuetzner, R. A.; Kuo, A.; Gulbis, J. M.; Cohen, S. L.; Chait, B. T.; MacKinnon, R. *Science* **1998**, *280*, 69–77.
- (100) Elcock, A.; Sept, D.; McCammon, J. *J. Phys. Chem. B* **2001**, *105*, 1504–1518.
- (101) Honig, B.; Nicholls, A. *Science* **1995**, *268*, 1144–1149.
- (102) Honig, B.; Hubbell, W. *Proc. Natl. Acad. Sci. U.S.A.* **1984**, *81*, 5412–5416.
- (103) Hendsch, Z.; Tidor, B. *Protein Sci.* **1994**, *3*, 211–226.
- (104) Yang, A.-S.; Honig, B. *J. Mol. Biol.* **1995**, *252*, 366–376.
- (105) Yang, A.-S.; Honig, B. *J. Mol. Biol.* **1995**, *252*, 351–365.
- (106) Schapira, M.; Totrov, M.; Abagyan, R. *J. Mol. Recognit.* **1999**, *12*, 177–190.
- (107) Luo, R.; David, L.; Hung, H.; Devaney, J.; Gilson, M. *J. Phys. Chem. B* **1999**, *103*, 727–736.
- (108) Froloff, N.; Windermuth, A.; Honig, B. *Protein Sci.* **1997**, *6*, 1293–1301.
- (109) Chong, L.; Dempster, S.; Hendsch, Z.; Lee, L.; Tidor, B. *Protein Sci.* **1998**, *7*, 206–210.
- (110) Lee, L.-P.; Tidor, B. *Protein Sci.* **2001**, *10*, 362–377.
- (111) Lee, L.-P.; Tidor, B. *Nat. Struct. Biol.* **2001**, *8*, 73–76.
- (112) Dong, F.; Vijayakumar, M.; Zhou, H. *Biophys. J.* **2003**, *85*, 49–60.
- (113) Wang, T.; Tomic, S.; Gabdoulline, R.; Wade, R. *Biophys. J.* **2004**, *87*, 1618–1630.
- (114) Warwicker, J.; Watson, H. *J. Mol. Biol.* **1982**, *157*, 671–679.
- (115) Gilson, M.; Sharp, K.; Honig, B. *J. Comput. Chem.* **1987**, *9*, 327–335.
- (116) Nicholls, A.; Honig, B. *J. Comput. Chem.* **1991**, *12*, 435–445.
- (117) Nina, M.; Beglov, D.; Roux, B. *J. Phys. Chem.* **1997**, *101*, 5239–5248.
- (118) Schreiber, G.; Fersht, A. R. *Biochemistry* **1993**, *32*, 5145–5150.
- (119) Kaminski, G. A.; Stern, H. A.; Berne, B. J.; Friesner, R. A.; Cao, Y. X.; Murphy, R. B.; Zhou, R.; Halgren, T. A. *J. Comput. Chem.* **2002**, *23*, 1515–1531.